Volume 5 • Issue 2

# AssayWise Letters

# Table of Contents

**Your Distributor:**
**BIOMOL GmbH**
Waidmannstraße 35
22769 Hamburg · Germany
info@biomol.de · www.biomol.de · www.biomol.com
Fon: +49 (0)40-853 260 0
Fax: +49 (0)40-853 260 22

TOLL FREE IN GERMANY:
Fon: 0800-246 66 51
Fax: 0800-246 66 52

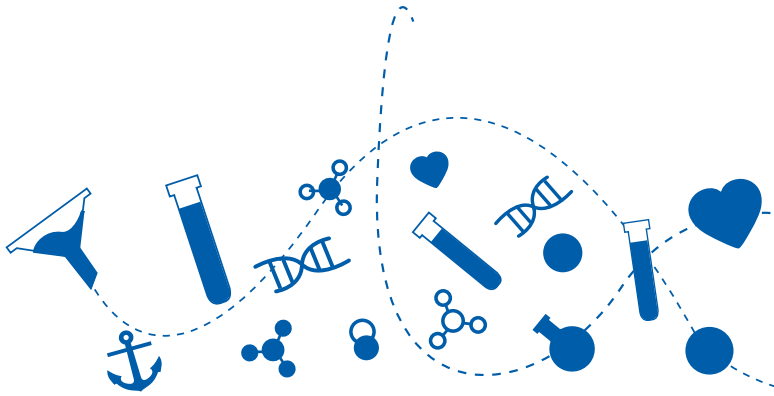

## Introducing Our Interactive Online Spectrum Viewer

Explore our extensive database of fluorescent dyes and proteins with the new Spectrum Viewer platform. With our interactive online Spectrum Viewer, you can:

- Easily view the spectra of our products
- Compare spectra from multiple fluorochromes
- Analyze excitation and emission values
- Determine spectral compatibilities and overlaps
- Choose the right dyes for multiplex assays

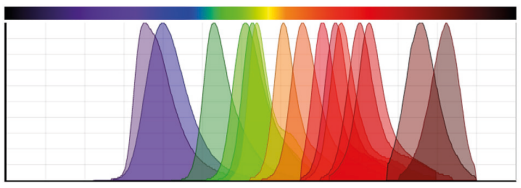

Our interactive online Spectrum Viewer is accessible from any web browser and is compatible with desktop, mobile and tablet devices. Access the Spectrum Viewer at https://www.aatbio.com/spectrum.

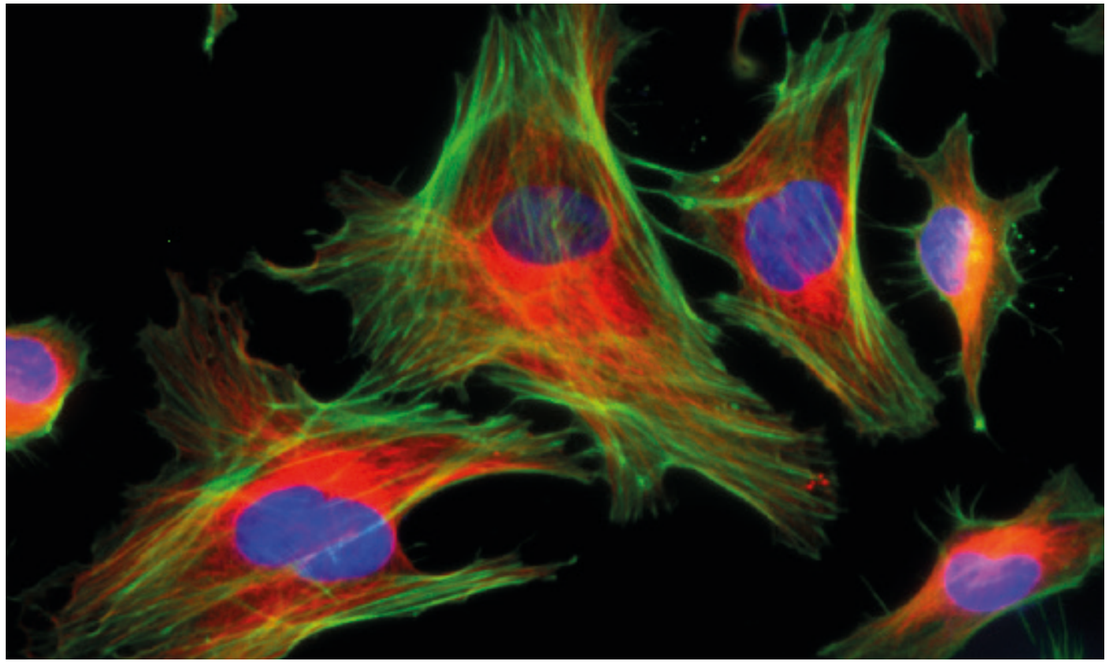

# Brighter Labeling with iFluor™ Conjugates

## Secondary antibodies conjugated with iFluor™ designed for robust and sensitive immunoassays

We are pleased to announce the release of two new product lines of secondary antibody conjugates. The first is a set of goat anti-mouse IgGs conjugates. The second uses goat anti-rabbit IgGs. Both sets of secondary antibodies have been conjugated with our superior iFluor™ fluorescent dyes. These secondary antibody conjugates are available in whole IgG format (H+L) and optionally cross-adsorbed (against human, swine and bovine IgG). Our goat anti-mouse IgG conjugates can also be optionally cross-adsorbed against rabbit and horse IgG, while our goat anti-rabbit IgG conjugates can also be optionally cross-adsorbed against mouse and rat IgG. Our iFluor™ secondary antibody conjugates are ideal for use in fluorescent western blotting, flow cytometry, fluorescent microscopy and fluorescent microplate readers. Our secondary antibody conjugates have undergone extensive testing and exhibit strong signal quality with minimal background staining. They have also been shown to be brighter than, and a good replacement for, Alexa Fluor® secondary antibody conjugates.

**Figure 1 (above).** HeLa cells were stained with mouse anti-tubulin followed with iFluor™ 633 Goat Anti-Mouse IgG (red, Cat# 16478), actin filaments were stained with Phalloidin-iFluor™ 488 Conjugate (green, Cat# 23115), and nuclei were stained with Hoechst 33342 (blue, Cat# 17530).







### It starts with high quality antibodies

Secondary antibodies, as a class, have become an essential component of a vast array of immunoassays. This is because, rather than targeting an antigen or protein directly, secondary antibodies target other (primary) antibodies. What this allows for is very efficient immunolabeling. Consider, instead of labeling each and every primary antibody, only a single secondary antibody (which targets afore mentioned primary antibodies) needs to be labeled. This translates into both saved time and reduced cost, two qualities that are essential in today's increasingly competitive industry.

Given the importance of secondary antibodies, it becomes vital to find the right one. In this regard, when researchers are asked, the majority will name specificity as the most important quality they look for when picking a secondary antibody. From a practical point of view, this makes a lot of sense. High specificity typically translates into better binding of the target substrate and less non-specific binding. What this means from an experimental perspective is that a highly specific secondary antibody results in stronger assay signals and lower noise.

The importance of high specificity extends beyond just secondary antibodies; it is of importance to secondary antibody conjugates as well. Recognizing this point, that high quality conjugates start with high quality antibodies, we have laid out an extensive quality control framework that validates our antibodies throughout the conjugation process. For a glimpse into our Quality Management System (QMS), here are a few steps we take to ensure the best quality antibodies:

1. Our host animals are carefully screened and undergo a validated immunization procedure with experimentally supported incubation times
2. Our total serum undergoes multiple rounds of affinity purification and dialysis to remove unwanted impurities and cell components
3. We offer cross-adsorbing of secondary antibodies to prevent cross-reaction with unwanted primary antibodies
4. Each lot of antibodies is tested through ELISA to ensure good activity before being passed to the conjugation process

Only antibodies that meet strict validation standards and show minimal nonspecific binding will pass our QMS and be used for conjugation. This guarantees that our customers receive the highest quality secondary antibody conjugates.

### It continues with superior labeling dyes

For the labeling dyes, we chose to use our superior iFluor™ product line. This is a series of fluorescent dyes known for their brightness and photostability, as well as their minimal quenching when bound to proteins. Our in-house testing has shown that even when the degree of substitution is high (that is, the dye to protein ratio is

**Table 1. iFluor™ Dye Equivalents of Common Dyes**

| If you are using | Try this iFluor™ dye |
|---|---|
| Alexa Fluor® 350, AMCA, DyLight™ 350 | iFluor™ 350 |
| Alexa Fluor® 405, DyLight™ 405 | iFluor™ 405 |
| Alexa Fluor® 488, Cy2®, FITC, DyLight™ 488 | iFluor™ 488 |
| Alexa Fluor® 514 | iFluor™ 514 |
| Alexa Fluor® 532 | iFluor™ 532 |
| Alexa Fluor® 555, Cy3®, DyLight™ 550, TRITC | iFluor™ 555 |
| Alexa Fluor® 594, DyLight™ 594, Texas Red® | iFluor™ 594 |
| Alexa Fluor® 633, DyLight™ 633 | iFluor™ 633 |
| Alxea Fluor® 647, Cy5®, DyLight™ 650 | iFluor™ 647 |
| Alexa Fluor® 680, Cy5.5®, IRDye® 700, DyLight™ 680 | iFluor™ 680 |
| Alexa Fluor® 700 | iFluor™ 700 |
| Alexa Fluor® 750, Cy7®, DyLight™ 750 | iFluor™ 750 |
| Alexa Fluor® 790, DyLight™ 800, IRDye® 800 | iFluor™ 790 |

high), these dyes will not show significant self-quenching, making them perfect for preparing secondary antibody conjugates.

In addition to minimized self-quenching, another reason we chose the iFluor™ product line is because these fluorescent dyes are fairly robust. Specifically, they can be used in a wide range of assay conditions. For example, iFluor™ 488 shows a stable signal across pH 4-10. This fluorescent stability under varying conditions allows for consistent assay results and flexibility in experimental design.

The last reason we chose the iFluor™ product line is because of its excellent fluorescence quantum yields. Broadly speaking, the fluorescence quantum yield is a measure of the number of photons emitted by a substance in relation to the number of photons it absorbed. When two compounds absorb identical amount of photons then, the one with the higher fluorescence quantum yield will emit more photons and appear brighter. Since our iFluor™ dyes have high fluorescence quantum yields, what this means is that under identical excitation conditions, our secondary antibody conjugates will outperform with better brightness.

Our iFluor™ product series comes in a wide array of excitations and emissions. At the moment, the product line consists of: iFluor™ 350, iFluor™ 405, iFluor™ 488, iFluor™ 514, iFluor™ 532, iFluor™ 555, iFluor™ 594, iFluor™ 610, iFluor™ 633, iFluor™ 647, iFluor™ 660, iFluor™ 680, iFluor™ 700, iFluor™ 750, iFluor™ 750 and iFluor™ 790, ranging the entire spectrum from UV to Near Infrared. Additionally, they are compatible with most standard lasers (eg. 488 nm argon-ion laser), allowing for easy adoption and convenient application.

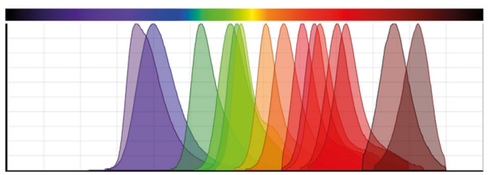

**Figure 2.** Emission spectra of iFluor™ product series generated using AAT Bioquest's Spectrum Viewer web application. iFluor™ dyes range from UV to Near Infrared (NIR). They are excellent for labeling antibodies, proteins and other biomolecules.

## It ends with conjugation and optimization

It starts with high quality antibodies. It continues with superior labeling dyes. It ends with conjugation and optimization.

What differentiates our secondary antibody conjugates from others on the market is our comprehensive conjugation and optimization process. Thanks to the collaborative efforts of our chemists and biologists, we are able to tailor our conjugation process to each antibody-dye pair, ensuring optimal results for each one of our conjugates individually. We accomplish this with several key steps.

First, we work to determine the ideal starting conditions for a particular antibody-dye conjugation. This includes developing the best buffer through fine tuning of buffer pH and ionic concentration, two factors which have been shown to influence the conjugation process. Additionally, we experimentally determine the ideal starting concentrations for both the antibody and the labeling dye. Ultimately, our goal for this optimization step is to optimize yield. Research has shown that an ideal starting condition greatly increases yield. An increased yield, in turn, translates into significant cost savings which we then pass to consumers.

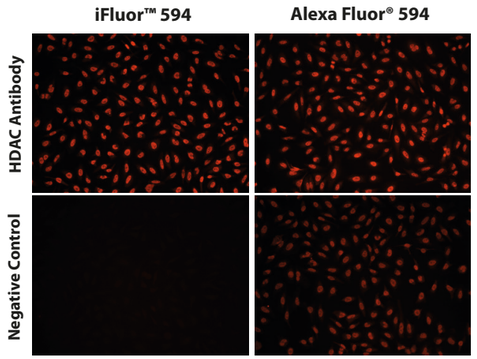


**Figure 3.** iFluor™ 594 gave much higher conjugation yield than Alexa Fluor® 594. HeLa cells were stained with Rabbit HDAC antibody, and then followed with iFluor™ 594 Goat Anti-Rabbit IgG Conjugate (Cat# 16628) and Alexa Fluor® 594 Goat Anti-Rabbit IgG Conjugate respectively under the same conditions. The iFluor™ 594 Goat Anti-Rabbit IgG Conjugate (left panel) demonstrated much lower staining background than the corresponding Alexa Fluor® 594 (right panel).

Second, we work to determine the ideal conjugation time. On the one hand, there needs to be enough time allotted for conjugation to occur. And not only occur, but occur with high yields which, as previously mentioned, translate into guaranteed cost savings for consumers. On the other hand, conjugation cannot be allowed to occur indefinitely even if it does lead to higher yields. At the very least, it would be impractical. But more importantly, it may lead to decreased antibody activity. That is why we find the sweet spot for conjugation time which maximizes yield while minimizing activity loss.







Third, and perhaps most importantly, we work to determine the ideal dye to antibody ratio, or degree of substitution (DOS). This, too, is a balance. Too little dye labeled onto the antibody leads to poor quality signals and poor brightness. Conversely, too much dye labeled onto the antibody can lead to a variety of problems as well, such as self-quenching, reduced affinity, higher background, poor conjugate solubility, poor conjugate loading and difficulty in usage.

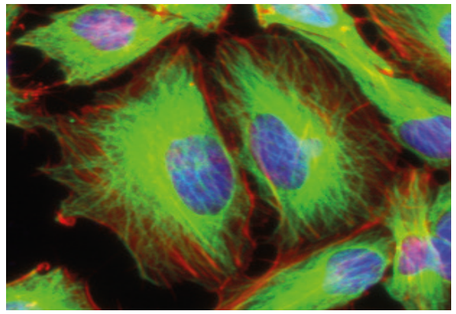

**Figure 4.** Image of HeLa cells. Tublins were stained with mouse anti-tubulin followed with iFluor™ 488 Goat Anti-Mouse IgG (green, Cat# 16448), actin filaments were stained with Phalloidin-iFluor™ 555 Conjugate (red, Cat# 23119), and nuclei were stained with Hoechst 33342 (blue, Cat# 17530).

That is why our conjugates are carefully prepared to be bright while still maintaining ease of use.

Finally, we work to determine the ideal purification process for our conjugates. Our purification process will remove unlabeled antibody as well as free, un-reacted dye. This is a vital step in the process for two reasons. First, unlabeled antibodies will compete with labeled antibodies for binding targets, but they will not produce a signal when bound. This leads to lower quality signals and lower brightness and must be minimized. Second, un-reacted free dye will increase the assay background. While this is detrimental for a variety of reasons, the most important is that it makes assay signals difficult to read and interpret, possibly masking the true positives while generating false ones. For these two reasons, optimal purification is essential to our conjugation process.

As you may have discovered, our optimization is not a single step, but rather, a comprehensive framework which spans the entire conjugation process. Ultimately, our goal is to provide the brightest secondary antibody conjugates at an affordable cost, that researchers may have a powerful tool for use in their studies. Below, you may find a sampling of our current conjugates.

**Table 2. iFluor™ Secondary Antibody Conjugates**

| Cat # | Product Name | Size | Ex (nm) | Em (nm) |
|---|---|---|---|---|
| 16448 | iFluor™ 488 Goat Anti-Mouse IgG (H+L) | 200 µg | 491 | 514 |
| 16528 | iFluor™ 488 Goat Anti-Mouse IgG (H+L) *Cross Adsorbed* | 200 µg | 491 | 514 |
| 16468 | iFluor™ 594 Goat Anti-Mouse IgG (H+L) | 200 µg | 592 | 614 |
| 16548 | iFluor™ 594 Goat Anti-Mouse IgG (H+L) *Cross Adsorbed* | 200 µg | 592 | 614 |
| 16478 | iFluor™ 633 Goat Anti-Mouse IgG (H+L) | 200 µg | 638 | 655 |
| 16558 | iFluor™ 633 Goat Anti-Mouse IgG (H+L) *Cross Adsorbed* | 200 µg | 638 | 655 |
| 16507 | iFluor™ 790 Goat Anti-Mouse IgG (H+L) | 200 µg | 782 | 811 |
| 16587 | iFluor™ 790 Goat Anti-Mouse IgG (H+L) *Cross Adsorbed* | 200 µg | 782 | 811 |
| 16608 | iFluor™ 488 Goat Anti-Rabbit IgG (H+L) | 200 µg | 491 | 514 |
| 16678 | iFluor™ 488 Goat Anti-Rabbit IgG (H+L) *Cross Adsorbed* | 200 µg | 491 | 514 |
| 16628 | iFluor™ 594 Goat Anti-Rabbit IgG (H+L) | 200 µg | 592 | 614 |
| 16698 | iFluor™ 594 Goat Anti-Rabbit IgG (H+L) *Cross Adsorbed* | 200 µg | 592 | 614 |
| 16638 | iFluor™ 633 Goat Anti-Rabbit IgG (H+L) | 200 µg | 638 | 655 |
| 16704 | iFluor™ 633 Goat Anti-Rabbit IgG (H+L) *Cross Adsorbed* | 200 µg | 638 | 655 |
| 16661 | iFluor™ 790 Goat Anti-Rabbit IgG (H+L) | 200 µg | 782 | 811 |
| 16721 | iFluor™ 790 Goat Anti-Rabbit IgG (H+L) *Cross Adsorbed* | 200 µg | 782 | 811 |
| 1255 | ReadiLink™ Rapid iFluor™ 488 Antibody Labeling Kit | 2 labelings | 491 | 514 |
| 1227 | ReadiLink™ Rapid iFluor™ 555 Antibody Labeling Kit | 2 labelings | 491 | 514 |

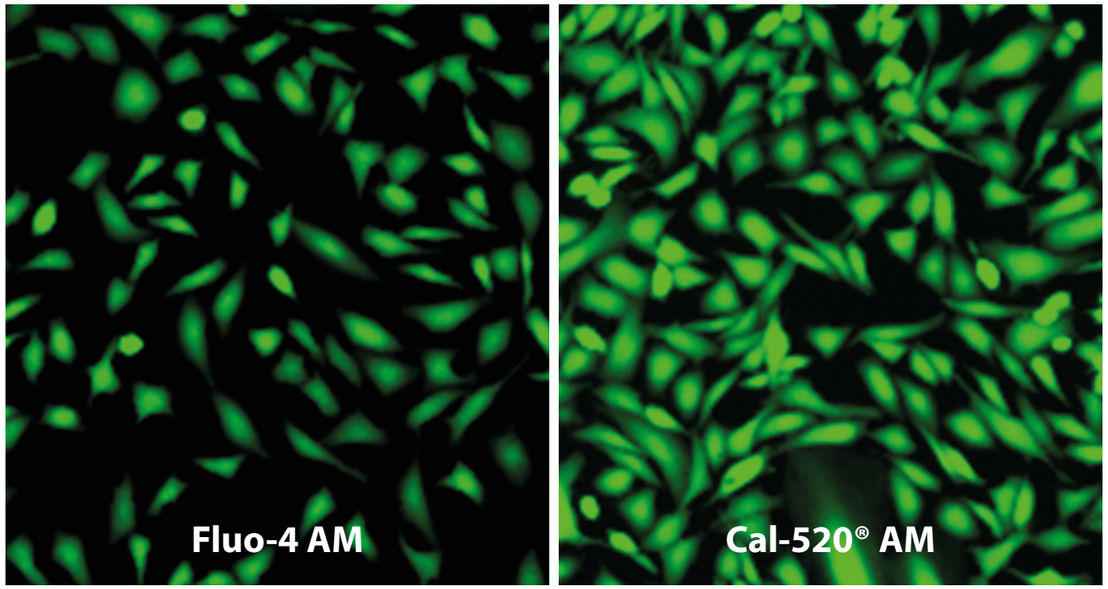


# Cal-520® AM

## The Development of a Low Background Calcium Indicator

### A History of Calcium Indicators

Every single year, hundreds of thousands of peer-reviewed papers are published focusing on calcium and its role in biological systems. The reason for this is clear. Calcium ion ($Ca^{2+}$) plays a critical role in many biological processes, from the contracting of muscles to the release of neurotransmitters. This pervasiveness of calcium in biology, and the subsequent need to study it, has made apparent the need for development of viable, convenient calcium indicators, tools that researchers may use to quantify and visualize intracellular calcium.

The first big breakthrough in calcium imaging came in the 1980s, when a team of scientists at the University of California Berkeley developed the first fluorescein-based calcium indicator. Their research paved the way for now well-established calcium probes, such as Fluo-3 AM and Fluo-4 AM. These hydrophobic, fluorescein-based AM esters readily pass through the membranes of living cells, where once inside, they are rapidly hydrolyzed by esterases and set to detect calcium. Upon successful binding with calcium, Fluo-3 or Fluo-4 will become fluorescent, emitting a signal at ~520 nm when excited by a ~490 nm light source.

**Figure 5 (above).** Responses of endogenous P2Y receptor to ATP in CHO-M1 cells with probenecid. CHO-M1 cells were seeded overnight at 40,000 cells per 100 µL per well in a Costar 96-well black wall/clear bottom plate. 100 µL of 4 µM Fluo-4 AM (left, Cat# 20552), Cal 520™ AM (right, Cat# 21130) in HHBS was added into the wells, and the cells were incubated at 37 °C for 2 hours. The dye loading medium was replaced with 100 µL HHBS and 50 µL of 300 µM ATP were added. The cells were imaged with a fluorescence microscope (Olympus IX71) using FITC channel.





Featured Product Spotlight

### Problems Abound

A significant achievement in its own right, these first generation fluorescein-based dyes did however suffer from several drawbacks. Most notably, these calcium probes were significantly affected by high background fluorescence, also known as noise. In general, researchers like to minimize background fluorescence as it creates many problems for bioassays and data analysis. It can obscure significant results and hide true positives while generating false signals, making interpretation of experimental responses incredibly difficult.

The severity of the background fluorescence generated by Fluo-3 AM and Fluo-4 AM has led to intense investigation into the matter, with researchers keying in on two likely causes. The first has to do with the chemical properties of acetoxymethyl (AM) esters. In solution, AM esters like Fluo-3 AM and Fluo-4 AM tend to hydrolyze, cleaving off the acetoxymethyl group. This means that when it comes time to load the dye into cells, a significant portion of the probe will be impermeable as they do not contain the AM functional group which allows them to pass through the cell membrane. This results not only in a lower fluorescence signal (as less dye permeated the cell), but also a higher background fluorescence as well. This is because the impermeable Fluo-3 or Fluo-4 outside the cell will still fluoresce and contribute to an elevated baseline fluorescence.

The second major cause of high background fluorescence is postulated to result from leakage of dyes through organic anion transports. It is assumed that Fluo-3 and Fluo-4 are poorly localized in the cytosol and can actually be transported into intracellular organelles or the extracellular matrix after being loaded into cells. This results in a situation similar to that of the hydrolyzed AM esters. That is, Fluo-3 or Fluo-4 will collect outside of the cell and fluoresce, again leading to an elevated baseline fluorescence. This is a particularly serious problem with calcium flux assays and calcium imaging as both depend on geospatial quantification of calcium. If the calcium probe itself is poorly localized and is being transported about, these bioassays become harder, if not impossible, to interpret.

### The Past Solution

After identifying that there was indeed a problem with current calcium indicators like Fluo-3 and Fluo-4, the first step we took was to investigate possible solutions already proposed in the industry. The best solution at the time was to utilize Fluo-3 and Fluo-4 in conjunction with a drug called probenecid.

Probenecid, as a drug, currently has two major uses. The first is to treat gout and hyperuricemia. The second is to prolong the effects of other drugs, such as penicillin. In both cases, the postulated mechanism of action is the same. That is, probenecid is hypothesized to target the kidneys wherein it inhibits organic anion transporter activity. This in turn causes greater retention of select compounds, such as pharmaceutical drugs, thereby prolonging their effects. This mechanism of action also explains the benefit to using probenecid in conjunction with Fluo-3 and Fluo-4. As you may recall, Fluo-3 and Fluo-4 can leak out of cells due to organic anion transporter activity. By inhibiting those transporters, probenecid leads to better Fluo-3 and Fluo-4 retention and consequently, lower background fluorescence.

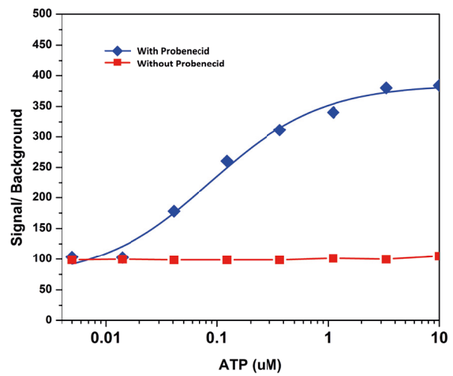


**Figure 6.** ATP-stimulated calcium response of endogenous P2Y receptor in CHO-K1 cells measured with Fluo-4 AM (Cat# 20552). CHO-K1cells were seeded overnight at 50,000 cells per 100 µL per well in a 96-well black wall/clear bottom Costar plate. 100 µL of 5 mM Fluo-4 AM with (blue) or without (red) 2.5 mM probenecid was added into the cells, and the cells were incubated at 37 °C for 1 hour. ATP (50 µL/well) was added by FlexStation® (Molecular Devices) to achieve the final indicated concentrations.

While probenecid was a good patchwork solution, we did not however find it a very satisfactory one. This was because we saw the benefits of probenecid usage as simultaneously its biggest flaw. That is, probenecid is a drug and, by its very nature, it alters cellular function. On the one hand, this means better cellular retention of calcium indicators. On the other, however, it means there is a whole host of yet unknown effects probenecid may have on cellular function (eg. increased cytotoxicity), leading to possible confounding variables. Furthermore, it introduces the need for additional controls (eg. probenecid dose), making it inconvenient to use.

### Our Development Process

Unsatisfied with the industry solution, we decided to seek our own to the background fluorescence problem. To this end, our process included three steps.

First, we conceptualized the solution and created an actionable goal. This involved our highly experienced chemists designing various alterations to the structure of Fluo-3 and Fluo-4. For example, one approach was to amend chemical properties to increase the stability of the AM ester bond. This would minimize hydrolysis in solution and improve cell loading. A second approach was to use functional groups to improve probe water solubility. By changing the chemical substituents, we sought to enhance cellular retention and improve localization. After a great deal of theoretical modeling, we were able to zero in on a few key structural changes that would solve the problem of high background fluorescence.

The next two steps will be familiar to anyone who has engaged in chemical production. It is the dual question of synthesis and scale. For us as a company, the question was not only how to produce our designed compound, but how to produce our designed compound efficiently. While optimal synthesis and scaling are both challenging and extremely hot topics of study in chemistry, it suffices to say that our teams of expert chemists were able to work out a reaction path with good yield. This was critical to our development process as good reaction paths drive down production costs and allow us to pass the savings to our customers. Combined with our strict Quality Management System, our efficient manufacturing process allows us to provide the highest quality products at the best values. This is a policy which we emphasize for all of our products, but particularly so during the development of our new calcium indicator. In the end, such a policy proved ideal. Our new calcium indicator, Cal-520® has been extremely successful in reducing background fluorescence, with customers reporting results that have even exceeded our own expectations.

### Features Aplenty

By making alterations to chemical structure, we significantly improved the stability of the AM ester bond. In AM ester form, Cal-520® AM shows very minimal spontaneous hydrolysis in solution when compared with Fluo-3 AM and Fluo-4 AM.

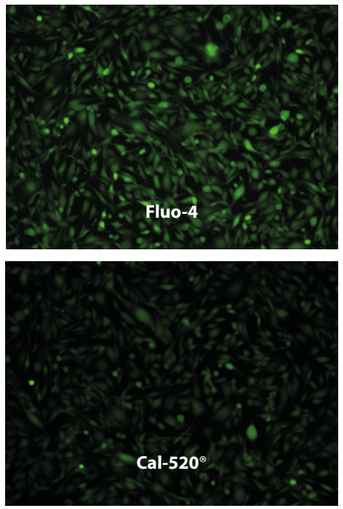


**Figure 7.** Background comparison of Fluo-4 AM (Cat# 20552) and Cal-520® AM (Cat# 21130). CHO-K1 cells were seeded overnight at 50,000 cells per 100 µL per well in a 96-well black wall/clear bottom Costar plate. 100 µL of 5 uM Fluo-4 AM or Cal-520® AM with probenecid was added into the cells and incubated at 37 ºC for 1 hour. After incubation, cells were washed once with HHBS and then background was imaged without ATP treatment.

Furthermore, we have optimized Cal-520®'s chemical structure so that it is better localized in cells. Unlike Rhod-2, which localizes in mitochondria, Cal-520® predominantly localizes in the cytosol. Additionally, once localized, it retains very well, even without the addition of probenecid. This is in huge contrast to Fluo-3 and Fluo-4. These features taken together mean lower background fluorescence and significantly improved signal to background ratio. Again, this is without the addition of probenecid or the need for constant washing of cells.

Furthermore, Cal-520® maintains the convenient spectra of Fluo-3 and Fluo-4. This allows for easy transition from older, outdated calcium indicators. There is no need to redesign experiment or purchase new equipment.

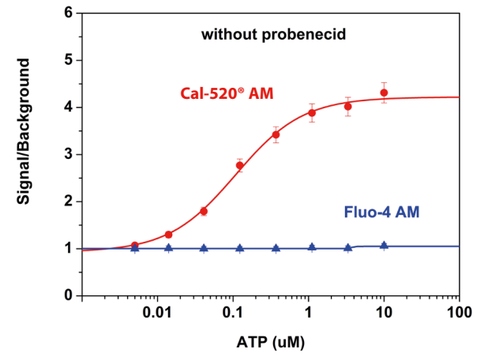


**Figure 8.** ATP-stimulated calcium responses of endogenous P2Y receptors in CHO-K1 cells incubated with Cal-520® AM (red curve, Cat# 21130), or Fluo-4 AM (blue curve, Cat# 20552) respectively, without probenecid under the same conditions. CHO-K1 cells were seeded overnight at 50,000 cells/100 µL/well in a Costar black wall/clear bottom 96-well plate. 100 µL of 5 µM Fluo-4 AM or Cal-520® AM in HHBS was added into the cells, and the cells were incubated at 37 °C for 2 hours. ATP (50 µL/well) was added using FlexSation® to achieve the final indicated concentrations.

**Table 3. Spectral Comparison of Fluo-3, Fluo-4, Fluo-8® and Cal-520®**

| Dye | Ex (nm) | Em (nm) | QY* |
|---|---|---|---|
| Cal-520® | 492 | 514 | **0.75** |
| Fluo-3 | 506 | 525 | 0.15 |
| Fluo-4 | 493 | 515 | 0.16 |

*QY = Fluorescence Quantum Yield in the presence of 5 mM calcium citrate.

Finally, we are excited to announce that we have adapted Cal-520® AM for easy application in multiplexing. For multiplexing, we have Cal-590™ AM and Cal-630™ AM, longer wavelength excitations that are completely compatible with green fluorescence indicators like GFP while maintaining the high signal to background ratio of Cal-520® AM.

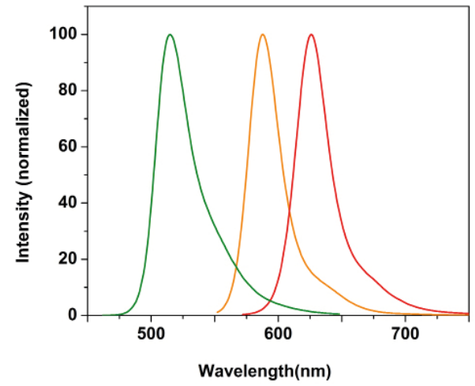


**Figure 9.** Normalized emission spectra of Cal-520® Green), Cal-590™ (Orange) and Cal-630™ (Red).

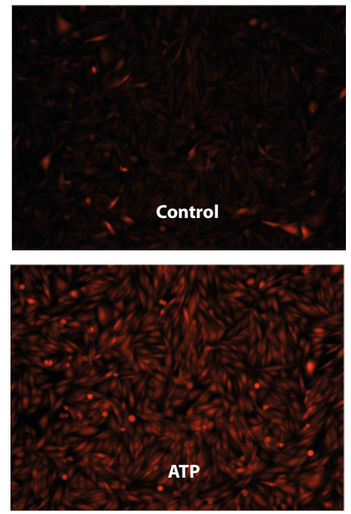


**Figure 10.** Responses of endogenous P2Y receptor to ATP in CHO-K1 cells. CHO-K1 cells were seeded overnight at 40,000 cells per 100 µL per well in a Costar 96-well black wall/clear bottom plate. 100 µL of 4 µM Cal-590™ AM (Cat# 20510) in HHBS with 1 mM probenecid were added into the wells, and the cells were incubated at 37 °C for 2 hours. The dye loading mediums were replaced with 100 µL HHBS and 1 mM probenecid, then imaged with a fluorescence microscope (Olympus IX71) using TRITC channel before and after adding 50 µL of 300 µM ATP .





For Pricing Information Please Visit: **www.biomol.de**

Unless otherwise specified, all products are for Research Use Only.
Not for use in diagnostic or therapeutic procedures.

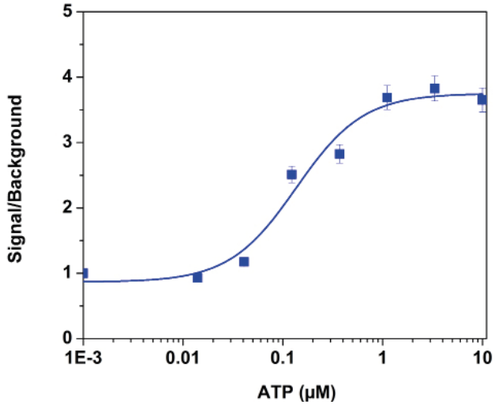


**Figure 11.** ATP-stimulated calcium response of endogenous P2Y receptor in CHO-K1 cells measured with Cal-630™ AM (Cat# 20530). CHO-K1 cells were seeded overnight at the cell density of 50,000 cells per 100 µL per well in a 96-well black wall/clear bottom plate. 100 µL of 10 µg/mL Cal-630™ AM with 2.0 mM probenecid was added into the cells, and the cells were incubated at 37 ºC for 2 hours. ATP (50 µL/well) was added by FlexStation® (Molecular Devices) to achieve the final indicated concentrations.

### Applications and Beyond

Because of Cal-520® AM's excellent chemical properties, it is a robust probe for fluorescence-based assay detection of intracellular calcium mobilization. It is perfect for evaluating GPCR and calcium channel targets as well as for screening their agonists and antagonists. Additionally, Cal-520® AM is completely compatible with use in flow cytometry, fluorescence microscopy, fluorescence spectroscopy and the fluorescence microplate platform.

As Cal-520® grows in popularity, we have seen it come to be cited in papers on a regular basis and in a variety of different fields, from neurobiology to cell signaling to cardiology. In particular, we are excited about the research currently being done by Tada et al. on monitoring single action potentials from neocortical neurons *in vivo*. We are also closely watching the research by Lock et al. on their investigation of long distance $Ca^{2+}$ communication via microtubules and regulation by inositol triphosphate (IP3). We are happy to see the adoption of Cal-520® by so many researchers, and we hope that Cal-520® will continue to be a powerful tool for researchers interested in studying intracellular calcium. For more information on Cal-520®, please check out our website at https://www.aatbio.com/products/cal-520 or email for inquiry at info@aatbio.com.

**Table 4. Classic Single Wavelength Fluorescent Calcium Indicators**

| Cat # | Product Name | Size | Ex (nm) | Em (nm) | $K_d$ |
|---|---|---|---|---|---|
| 21140 | Cal-520®, Potassium Salt | 10x50 µg | 492 | 514 | 320 nM |
| 21144 | Cal-520FF™, Potassium Salt | 10x50 µg | 492 | 514 | 9.8 µM |
| 20518 | Cal-590™, Potassium Salt | 5x50 µg | 573 | 588 | 561 nM |
| 20538 | Cal-630™, Potassium Salt | 5x50 µg | 608 | 626 | 792 nM |
| 20500 | Cal Green™ 1, Hexapotassium Salt | 10x50 µg | 506 | 531 | 190 nM |
| 21017 | Fluo-3, Pentapotassium Salt | 1 mg | 506 | 526 | 390 nM |
| 21019 | Fluo-3FF, Pentapotassium Salt | 1 mg | 506 | 526 | 10 µM |
| 20556 | Fluo-4, Pentapotassium Salt | 10x50 µg | 494 | 516 | 345 nM |
| 21089 | Fluo-8®, Potassium Salt | 10x50 µg | 494 | 517 | 389 nM |
| 21102 | Fluo-8FF™, Potassium Salt | 10x50 µg | 494 | 517 | 10 µM |
| 21100 | Fluo-8L™, Potassium Salt | 10x50 µg | 494 | 517 | 1.9 µM |
| 21067 | Rhod-2, Tripotassium Salt | 1 mg | 549 | 578 | 570 nM |
| 21129 | Rhod-4™, Potassium Salt | 5x50 µg | 524 | 551 | 451 nM |
| 21072 | Rhod-5N, Tripotassium Salt | 1 mg | 551 | 577 | 0.3 mM |
| 21075 | Rhod-FF, Tripotassium Salt | 1 mg | 549 | 578 | 19 µM |







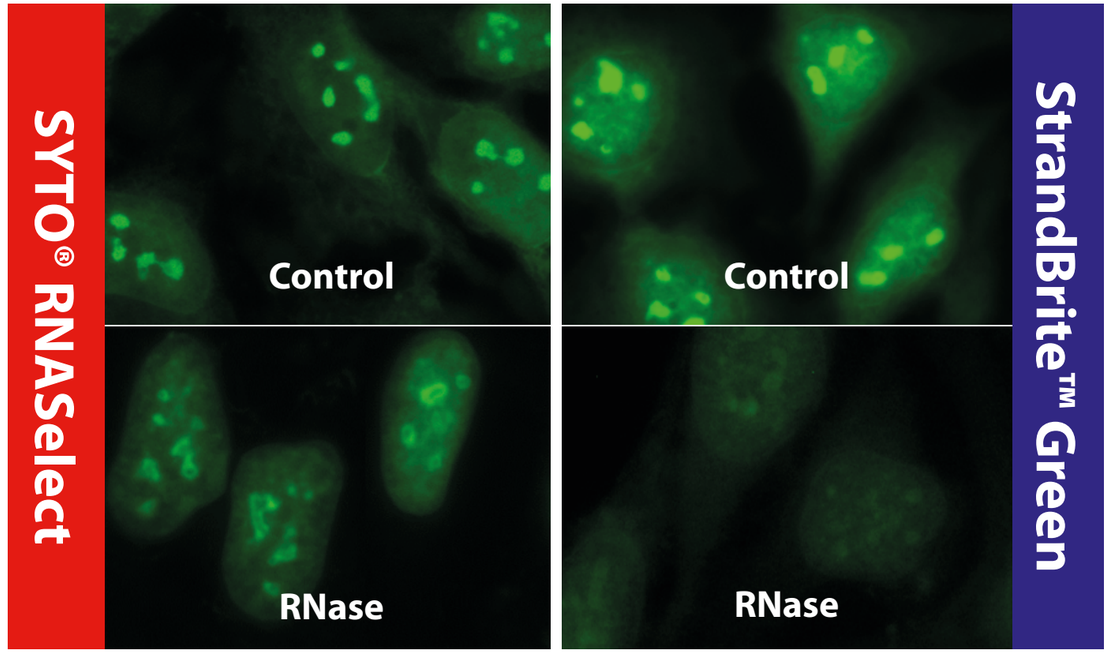


# Advances in Nucleic Acid Detection

## An Overview of Current Tools for DNA and RNA Quantification

### A History of DNA Detection

When discussing nucleic acid detection, there are two components to keep in mind: the detector and the transducer. The detector is the part which recognizes the nucleic acid and interacts directly with it. The transducer is the part which then generates a quantifiable signal from that interaction. Take, for example, the well-developed DNA detection method called fluorescence in situ hybridization (FISH).

FISH was first developed in the 1980s as a method to detect specific sequences of DNA on chromosomes. It works by designing a single stranded DNA (ssDNA) probe that is complementary to the target sequence. The probe needs to have enough base pairs to bind specifically to the target sequence while small enough to not interfere with hybridization. Once a probe, or detector, is designed, it is then tagged with a fluorophore which acts as a signal transducer and allows for sequence detection events to be quantified. With the probe prepared, the sample DNA is denatured, and the probe is added. As the DNA anneals, hybridization will occur, wherein the probe and the target ssDNA will combine to reform double stranded DNA (dsDNA). Then the probe, and consequently the target DNA sequence, can be detected using standard instrumentation, such as fluorescent microscopy.

**Figure 12 (above).** Fluorescence images of RNA staining taken in HeLa cells with SYTO® RNASelect (left, trademark Invitrogen) and StrandBrite™ Green (right). Cells were fixed in methanol and imaged using a fluorescence microscope with a FITC filter (control). After staining, fixed HeLa cells were incubated with 0.5 mg/mL RNase at 37˚C for 1 hour (RNase). Image of RNase digest test indicates the high selectivity of StrandBrite™ Green.

While an elegant method, several considerations have to be made when using FISH and similar hybridization procedures. For example, competition between probe and sample DNA will reduce successful hybridization during annealing, leading to dsDNA comprised only of sample ssDNA. The exclusion of the probe in dsDNA will have a significant impact on signal quality. Furthermore, FISH does not reflect live cell conditions. DNA is denatured at temperatures well above that of cellular environments, and in fact, the very denaturing requirement itself poorly reflects actual cell conditions. Most DNA in cells persists as dsDNA rather than ssDNA.

Aside from cellular conditions, there are practical issues to consider. For example, FISH is a very time consuming procedure, requiring approximately 12 hours per assay. Often times, researchers simply want a quick assay to quantify DNA, without necessarily targeting specific sequences. For these types of applications, a vast array of probes has been developed that not only offer convenience of use but also detection of dsDNA without extreme denaturing procedures.

### dsDNA Detection

If specific sequence detection is not required, then there are many chemical probes available for detection of dsDNA. One of the earliest was 4′,6-diamidino-2-phenylindole (DAPI).

DAPI was first developed in 1971, and it is still used extensively in fluorescence microscopy. It acts by binding to AT rich regions of dsDNA. Once bound to dsDNA, it will emit a strong signal at 461 nm when excited by an ultraviolet light source (maximal absorption at 358 nm). Because DAPI is cell permeable, it can theoretically be used to stain both fixed and live cells. It is, however, worth noting that DAPI is less permeable in live cells and thus stains much more poorly than in fixed cells.

Another commonly used chemical probe is the bisbenzimides family. Of these, the Hoechst stains are the most well established. Like DAPI, the Hoechst stains will bind to AT rich regions in dsDNA, localizing in the minor groove. The Hoechst stains have two significant advantages over DAPI, however. First, the Hoechst dyes have an extra ethyl group in their chemical structure, which makes these compounds more hydrophobic. This allows for easier access through the cell membrane of live cells and, consequently, better staining. Second, the Hoechst stains tend to be less toxic, which minimizes their impact on cellular function. This once again benefits the staining of live cells. Of the Hoechst stains, Hoechst 33258 and Hoechst 33342 are the most commonly used. These two dyes are similar in that they both excite at around 350 nm and emit a blue/cyan fluorescent light with a maximum emission at about 460 nm. Because of their spectra, they tend to act as a good replacement for DAPI.

More recently, there has been intense focus on developing probes that have greater sensitivity and selectivity for dsDNA. In particular, it is worth mentioning the development of Helixyte™ Green. Like DAPI and the Hoechst probes, Helixyte™ Green binds to the minor groove of DNA. However, it has significant improvements over these first-generation dsDNA dyes. First, Helixtye™ Green is significantly more selective. Unlike DAPI, it has very minimal binding to RNA. And in comparison to Hoechst 33258, Helixyte™ Green also shows improved binding to homopolymers, regions of dsDNA which have repeating base pairs (eg. AAAA, TTT). In terms of sensitivity, Helixyte™ Green is purportedly one of the most sensitive probes for quantifying dsDNA in solution. According to its specifications, Helixyte™ Green will selectively detect as little as 25 pg/mL dsDNA even in the presence of ssDNA, RNA and free nucleotides. This makes it roughly 400 times more sensitive than Hoechst 33258 under the same dye concentrations. Finally, Helixyte™ Green is reported to have linearity across three orders of magnitude. This is in reference to the linearity of dilution assessment. In short, it means that assay functionality does not deviate significantly under different analyte dilutions. This translates into a robust assay with high precision across a wide range of experimental conditions and allows for quantification of DNA from a variety of sources including genomic DNA, viral DNA, miniprep DNA and PCR amplification products.

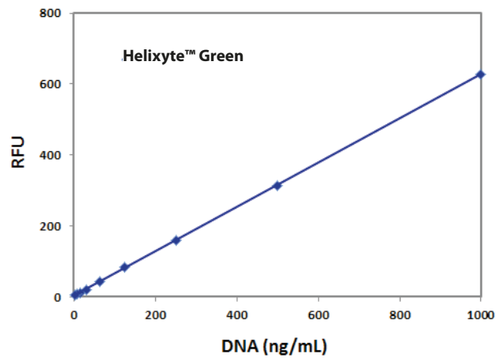


**Figure 13.** Calf thymus DNA dose response with Helixyte Green™ in a solid black 96-well microplate using a Gemini fluorescence microplate reader.







In addition to creating probes with greater sensitivity and selectivity for dsDNA, researchers have been keen to make dsDNA probes available for multiplex assays. For example, Nuclear Blue™ DCS1, a DNA-selective and cell-impermeant fluorogenic dye, has found great success in applications involving fixed, GFP cell lines. Analogous dyes, such as Nuclear Orange™ DCS1 and Nuclear Red™ DCS1, have also become available and offer solutions for applications which require longer wavelength probes.

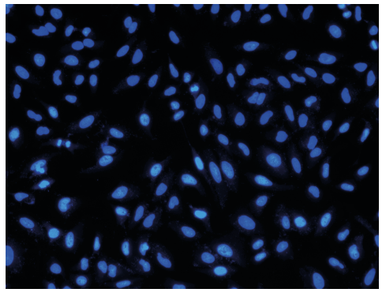

**Figure 14.** Dead cell imaging with Nuclear Blue™ DCS1 (Cat# 17548). Fixed HeLa cells plated on 96-well plates, incubated with 2.5 µM Nuclear Blue™ DCS1 (Cat# 17548) for 20 minutes and imaged with DAPI channel.

### RNA Detection

With clear advances in dsDNA detection, it is worth mentioning that there have been significant strides in RNA detection as well. In particular, StrandBrite™ Green has generated impressive results. StrandBrite™ Green is a fluorescent probe that is capable of detecting as little as 5 ng/mL of RNA in assay solution through use of instrumentation such as fluorescence microplate readers. To determine RNA selectivity, a standard DNase and RNase digest test was conducted. After DNase digestion, it was found that fixed cells stained with StrandBrite™ Green did not experience a significant change in initial fluorescence intensity. On the other hand, after RNase digestion, there was an immediate and dramatic decrease of initial fluorescence signal. Furthermore, short exposure of live cells to dantinomycin caused dose-dependent detection of inhibited RNA synthesis during the 6 hours after drug removal. All of these results strongly support the claim that fluorescence signals derived from StrandBrite™ Green are a result of specific interactions between the probe and RNA in sample cells.

Due to its excellent cell permeability and spectral properties, StrandBrite™ Green has been successfully used for flow cytometry-based RNA analysis and fluorescence microscopy in live cells. It is well excited by 488 nm argon-ion lasers and uses the standard FITC channel emission filter, making it a convenient and valuable tool for the quantification of RNA.

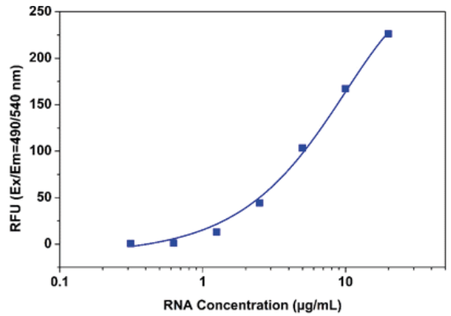


**Figure 15.** RNA dose response with StrandBrite™ Green Fluorimetric RNA Qutantitation Kit *High Selectivity* (Cat# 17657) in a solid black 96-well microplate using a Germini microplate reader (Molecular Devices).

### Table 5. Product Ordering Information

| Cat # | Product Name | Size | Ex (nm) | Em (nm) |
|---|---|---|---|---|
| 17510 | DAPI [4,6-Diamidino-2-phenylindole, dihydrochloride] *CAS# 28718-90-3* | 1 mg | 358 | 461 |
| 17597 | Helixyte™ Green dsDNA Quantifying Reagent *200X DMSO Solution* | 1 mL | 501 | 520 |
| 17651 | Helixyte™ Green Fluorimetric dsDNA Quantitation Kit *High Sensitivity* | 200 tests | 501 | 520 |
| 17650 | Helixyte™ Green Fluorimetric dsDNA Quantitation Kit *Optimized for Microplate Readers* | 200 tests | 501 | 520 |
| 17530 | Hoechst 33342 *CAS# 23491-52-3* | 100 mg | 350 | 461 |
| 17548 | Nuclear Blue™ DCS1 | 0.5 mL | 350 | 461 |
| 17551 | Nuclear Orange™ DCS1 | 0.5 mL | 528 | 576 |
| 17552 | Nuclear Red™ DCS1 | 0.5 mL | 642 | 660 |
| 17656 | StrandBrite™ Green Fluorimetric RNA Quantitation Kit | 100 tests | 500 | 525 |
| 17657 | StrandBrite™ Green Fluorimetric RNA Quantitation Kit *High Selectivity* | 100 tests | 508 | 528 |
| 17655 | StrandBrite™ Green Fluorimetric RNA Quantitation Kit *Optimized for Microplate Readers* | 1,000 tests | 500 | 525 |

# Hydrogen Peroxide and Salt-Sensitive Hypertension

*Too much salt will raise your blood pressure*

This statement has been repeated with enough frequency that it has become a colloquialism. It has sparked intense debate amongst researchers in the science community as well as in the general public, with many swearing by the statement and with others pointing out that the effects are minimal at best. This wealth of interest has spurred decades of research into the matter, with mounting evidence suggesting that salt does in fact contribute to hypertension- for some. These individuals, so-described as salt-sensitive, will indeed experience elevated blood pressure that correlates with their dietary salt intake. This poses a problem as long term hypertension can lead to a variety of health concerns such as coronary artery disease, stroke and heart failure. With cardiovascular disease still the leading cause of death in the United States, researchers have turned a closer eye towards salt-sensitive hypertension in the hopes of understanding its pathology and developing future therapies.

Early work on salt-sensitive hypertension suggested that it affects a heterogeneous population of individuals, though possibly weighted towards certain demographic factors such as age and gender. It has also been postulated that there is a genetic component to salt-sensitive hypertension as it seemed more frequent in individuals with a family history of high blood pressure. In terms of actual physiology, a variety of candidates have been suggested as contributing to salt sensitivity, from the renin-angiotensin-aldosterone system to blood insulin levels. More recently, researchers have narrowed in on a system of epithelial sodium channels in the renal cortex, hypothesizing that the function of these channels are at the crux of the matter.

Epithelial sodium channels (ENaC) are membrane-bound ion-channels found in the kidneys and are responsible for reabsorption of sodium ions. It has been suggested that excess reabsorption by these channels is directly linked to the expression of salt-sensitive hypertension. For example, in a paper published in 2000 by Gariepy et al., it was found that the lack of tonic inhibition of ENaC led to severe hypertension in rats with high sodium diets while rats with low sodium diets did not develop the condition. Many papers published since have also alluded to the development of salt-sensitive hypertension stemming from increased ENaC activity.

More recently, several papers have been published indicating that the upregulation of ENaC is a result of oxidative stress, mediated by the cellular secondary messenger hydrogen peroxide ($H_2O_2$). For a long time, $H_2O_2$ was viewed as merely toxic waste resulting from aerobic metabolism. It was considered damaging to cells because of its ability to induce breaks in single stranded and double stranded DNA amongst other things. Further investigation, however, has uncovered that $H_2O_2$ is actually involved in a complex array of redox pathways involving NOX (NADPH oxidase complex) and glutathione peroxidase. These redox mechanisms not only manage oxidative stress in cells, but also serve to regulate many signal transduction pathways through phosphorylation of key signaling proteins. With regards to salt-sensitive hypertension, many researchers believe $H_2O_2$ is the key to understanding the regulation of ENaC.

There are several reasons to believe that $H_2O_2$ may modulate ENaC activity. First, $H_2O_2$ is already known to regulate the function of several transmembrane proteins such as ATP-sensitive potassium channels. Second, studies in transgenic mice have found that increased catalase activity, which decomposes $H_2O_2$ into water and oxygen, is correlated with a decrease in sensitivity to hypertension inducing agents. Finally, studies on Tempol, an antioxidant which reduces renal oxidative stress, suggest that long term treatment prevents expression of hypertension. In more direct testing, it was found that $H_2O_2$ might regulate ENaC activity through phosphatidylinositide 3-kinase (PI3K). In A6 distal nephron cells, the addition of $H_2O_2$ led to increased ENaC open probability, which allowed for increased $Na^+$ reuptake. However, upon inhibition of PI3K, ENaC open probability as well as $Na^+$ uptake reverted to pre-$H_2O_2$ levels. This would seem to suggest that $H_2O_2$ not only plays a critical role in $Na^+$ reabsorption, but does so through a kinase (PI3K) which is consistent with previous studies on $H_2O_2$ mechanism as a secondary messenger. If $H_2O_2$ is the mediator for ENaC activity, it is worth doing further investigation in the hopes of developing treatments for salt-sensitive hypertension.







## Our Tools

We offer several tools to help researchers accurately study $H_2O_2$ and its related compounds. For example, in a study published in the *Journal of Biological Chemistry*, our Amplite™ Fluorimetric Hydrogen Peroxide Assay Kit was used to quantify $H_2O_2$ concentration in A6 distal nephron cells. This assay kit uses our Amplite™ Red peroxidase substrate to quantify $H_2O_2$ in solution and cell extracts through enzyme-coupled reactions. It is a one step assay that can detect as little as 3 pmol of $H_2O_2$ in a 100 uL assay volume. It can be conveniently applied in a 96-well or 384-well plate and be read in a fluorescence microplate reader. We offer this kit in red, near red and green fluorescence for experimental flexibility and easy multiplexing. Because these kits are a simple mix-and-read assay, they can be easily adaptable to HTS liquid handling instruments and usable for automation.

We additionally offer Cell Meter™ Intracellular Fluorimetric Hydrogen Peroxide Assay Kits for live cell applications. These kits use our OxiVision™ peroxide sensor. This is a cell-permeable probe that will generate a fluorescence signal upon reaction with $H_2O_2$. The probe comes in two versions, blue fluorescence and green fluorescence. Our blue fluorescence probe excites at 405 nm and emits at 450 nm, while our green fluorescence probe excites at 490 nm and emits at 530 nm. We also have kits optimized for flow cytometry applications.

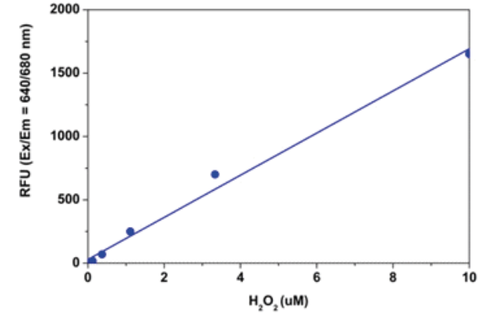


**Figure 16.** $H_2O_2$ dose response was measured in a solid black 96-well plate with Amplite™ Fluorimetric Hydrogen Peroxide Assay Kit (Cat# 11502). As little as 0.03 µM $H_2O_2$ was detected.

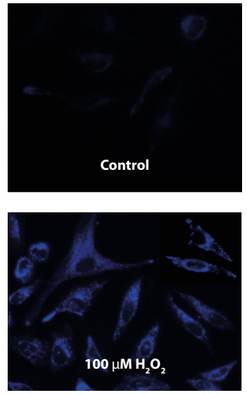


**Figure 17.** Fluorescence images of intercelluar hydrogen peroxide in HeLa cells using Cell Meter™ Intercellular Fluorimetric Hydrogen Peroxide Assay Kit (Cat# 11504). HeLa cells were stained with OxiVision™ Blue peroxide sensor for 30 minutes and treated with (bottom) or without (top) 100 µM hydrogen peroxide at 37 ºC for 90 minutes.

In addition to our hydrogen peroxide detectors, we also provide glutathione assay kits for life science researchers. This category of kits includes assays for the quantification of GSH/GSSG ratio as well as total glutathione. This allows for easy characterization of cellular oxidative stress. Our kits are all mix-and-read, meaning that no separation step is required. This enables quick application with minimal hands-on-time. These assays are ultra-sensitive, with the ability to detect as little as 1 pmol of GSH in a 100 uL of assay volume. Our kits are compatible with standard microplate readers (Ex/Em = 490/520 nm).

**Table 6. Product Ordering Information**

| Cat # | Product Name | Size | Ex (nm) | Em (nm) |
|---|---|---|---|---|
| 11502 | Amplite™ Fluorimetric Hydrogen Peroxide Assay Kit *Near Infrared Fluorescence* | 500 tests | 647 | 670 |
| 11501 | Amplite™ Fluorimetric Hydrogen Peroxide Assay Kit *Red Fluorescence* | 500 tests | 575 | 590 |
| 11504 | Cell Meter™ Intracellular Fluorimetric Hydrogen Peroxide Assay Kit *Blue Fluorescence* | 100 tests | 405 | 450 |
| 11505 | Cell Meter™ Intracellular Fluorimetric Hydrogen Peroxide Assay Kit *Blue Fluorescence Optimized for Flow Cytometry* | 100 tests | 405 | 450 |
| 11506 | Cell Meter™ Intracellular Fluorimetric Hydrogen Peroxide Assay Kit *Green Fluorescence Optimized for Flow Cytometry* | 100 tests | 490 | 530 |

# A Look at NAD-Dependent SIRT1

It has long been suspected that SIRT1 plays a role in modulating cellular metabolism. For example, early studies showed that SIRT1 is critical to the regulation of glucose homeostasis through regulation of gluconeogenic and glycolyic pathways. Specifically, a study by Rodgers et al. found that SIRT1 interacts with a transcriptional cofactor called PGC-1α. Through the deacetylation of PGC-1α at lysine residues, SIRT1 is able to induce gluconeogenic genes, which leads to increases in glucose output in hepatic cells. Additional studies have supported these initial findings, with research showing that SIRT1 acts as a metabolic switch in cardiac and skeletal myocytes amongst other cell lines.

While it seems fairly evident that SIRT1 plays a role in modulating cellular metabolism, what is much more controversial is the idea that SIRT1 plays a role in cellular longevity and aging. In particular, a wealth of research seems to suggest that caloric restriction, or fasting, will activate SIRT1 pathways and lead to lifespan extension. Such findings have spanned different kingdoms, with the effects of caloric restriction present in organisms like yeast, flies and rats. Such findings have also prompted a frenzy of research into the potential links between caloric restriction, SIRT1 and neurodegenerative diseases like Alzheimer's dementia. The increased interest in caloric restriction has led many researchers to investigate the possible mechanisms in which SIRT1 may be involved.

Research by Brunet et al. in 2004 seems to suggest that SIRT1 may play a role in the regulation of FOX (Forkhead box) transcription factors, particularly one called FOXO3. The FOX proteins are well-known to have important influences on genes regulating cell growth, proliferation and apoptosis, so it is certainly a possible pathway by which SIRT1 can modulate cell longevity. Brunet et al. argue that SIRT1 acts to deacetylate FOXO3, which in experiments resulted in increased cellular resistance to oxidative stress while simultaneously inhibiting induced cell death. The overall effect, they posit, is an increase in cell longevity.

While FOXO3 may be the mechanism by which SIRT1 leads to lifespan extension, it does not explain why caloric restriction specifically will lead to activation of FOX pathways. For this, many researchers have pointed to studies in *S. cerevisiae*. In particular, researchers have argued that SIRT1's NAD-dependent activation is the link between caloric restriction and lifespan extension. In *S. cerevisiae*, caloric restriction causes a metabolic shift in which the more efficient respiration pathway becomes preferred over the less efficient fermentation pathway. This change in metabolic pathway causes an alteration in the NAD+/NADH ratio, leading to an increase in cellular NAD+, an increase in SIRT1 activity and, as researchers have argued, an increase in cell longevity. More recently, however, some contradictory evidence has arisen which seems to at least cast doubt onto this explanation. For example, in *S. cerevisiae*, which are unable to undergo respiration, the same correlation between caloric restriction and longevity has been found. Studies in worms have also found that reduced mitochondrial function is correlated with increases in lifespan. This has motivated many researchers to seek alternative explanations for the link between caloric restriction and SIRT1 up-regulation, with many suggesting that NAD+ regeneration from nicotinamide (NAM) should receive closer investigation.

## Our Tools

We offer an extensive catalog of kits for life science researchers interested in studying NAD and NADH. These kits come in two varieties: colorimetric and fluorimetric. In general, we recommend fluorimetric kits as these tend to be more sensitive. However, many researchers may prefer colorimetric kits due to compatibility with existing equipments. Fluorimetric kits will require a fluorescence microplate reader or analogous setup. Colorimetric kits can be read with standard absorbance microplate readers.

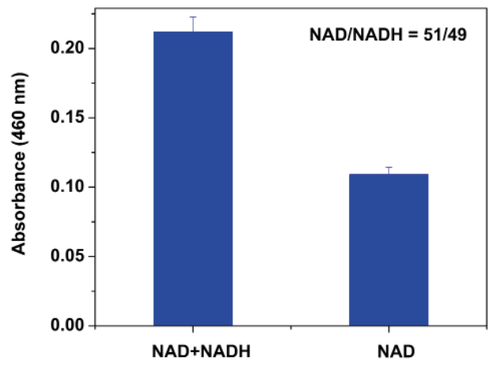


**Figure 18.** Amplite™ Colorimetric NAD/NADH Ratio Assay Kit (Cat#15273) was used to measure NAD/NADH ratio in a 96-well white wall/clear bottom microplate using a SpectraMax® microplate reader (Molecular Devices). Equal amount of NAD and NADH mixtures were treated with or without NAD extraction solution for 15 minutes, and then neutralized with extraction solution at room temperature. The signal was read at 460 nm. NAD/NADH ratio was calculated based on the absorbances shown in the figure.

Our colorimetric assay kits utilize a novel chromogenic sensor that is superior to traditional NAD/NADH probes. Unlike traditional probes which maximally absorb at 340 nm, our probe has a maximum absorbance at 460 nm upon NADH reduction. This means that it does not require the use of quartz microplates, which are not only expensive but tend to result in low sensitivity and high interference. The concentration of NADH in a sample solution can easily be calculated from the absorbance at 460 nm as these two values are proportional. Our probe is sensitive enough that it can detect as little as 3 µM NADH in a 100 µL assay volume and is excellent for studies involving oxidative stress in which the NAD/NADH system is involved.

For fluorimetric detection, we have our Amplite™ Fluorimetric NAD/NADH Ratio Assay Kit *Red Fluorescence*. This kit consists of a system of enzymes that specifically recognize NAD/NADH through use of an enzyme cycling reaction. Compared with other detection methods, our enzyme cycling reaction significantly increases detection sensitivity. In addition, this assay has been shown to have very low background. This is due to its spectral properties, which lie in the red visible range, significantly reducing interference from biological samples. For researchers concerned about usability, our kit is very convenient in its application. There is no need to purify NAD/NADH from the sample prior to use; simply mix-and-read using a fluorescence microplate reader (Ex/Em = 540/590 nm).

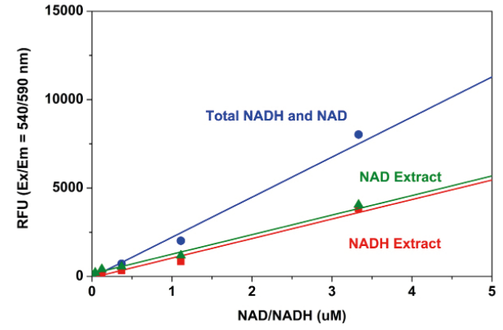


**Figure 19.** Total NAD and NADH, and their extract dose responses were measured with Amplite™ Fluorimetric NAD/NADH Ratio Assay Kit (Cat# 15263) in a 96-well black plate. 25 µL of equal amount of NAD and NADH was treated with or without NADH or NAD extraction solution for 15 minutes, and then neutralized with extraction solutions at room temperature. The signal was acquired at Ex/Em = 540/590 nm (cut off at 570 nm) 30 minutes after adding 75 µL NADH reaction mixture. The blank signal was subtracted from the values of those wells with the NADH reactions.

**Table 7. NAD/NADH & NADP/NADPH Assay Comparison**

| Cat. # | Product Name | Assay Target | Detection Mode | Detection Limit | Dynamic Range |
|---|---|---|---|---|---|
| 15280 | Amplite™ Fluorimetric NAD Assay Kit *Blue Fluorescence* | NAD | Fluorescence | 0.03 µM | 0.03-10 µM |
| 15271 | Amplite™ Colorimetric NADH Assay Kit | NADH | Absorption | 3 µM | 1-200 µM |
| 15261 | Amplite™ Fluorimetric NADH Assay Kit *Red Fluorescence* | NADH | Fluorescence | 1 µM | 0-100 µM |
| 15258 | Amplite™ Colorimetric Total NAD and NADH Assay Kit | NAD+NADH | Absorption | 0.3 µM | 0-10 µM |
| 15275 | Amplite™ Colorimetric Total NAD and NADH Assay Kit *Enhanced Sensitivity* | NAD+NADH | Absorption | 0.1 µM | 0.1-10 µM |
| 15257 | Amplite™ Fluorimetric Total NAD and NADH Assay Kit *Red Fluorescence* | NAD+NADH | Fluorescence | 0.1 µM | 0-3 µM |
| 15273 | Amplite™ Colorimetric NAD/NADH Ratio Assay Kit | NAD/NADH Ratio | Absorption | 0.1 µM | 0.1-10 µM |
| 15263 | Amplite™ Fluorimetric NAD/NADH Ratio Assay Kit | NAD/NADH Ratio | Fluorescence | 0.1 µM | 0-3 µM |
| 15281 | Amplite™ Fluorimetric NADP Assay Kit *Blue Fluorescence* | NADP | Fluorescence | 0.03 µM | 0.03-10 µM |
| 15272 | Amplite™ Colorimetric NADPH Assay Kit | NADPH | Absorption | 3 µM | 1-200 µM |
| 15262 | Amplite™ Fluorimetric NADPH Assay Kit *Red Fluorescence* | NADPH | Fluorescence | 1 µM | 0-100 µM |
| 15260 | Amplite™ Colorimetric Total NADP and NADPH Assay Kit | NADP+NADPH | Absorption | 0.1 µM | 0-3 µM |
| 15276 | Amplite™ Colorimetric Total NADP and NADPH Assay Kit *Enhanced Sensitivity* | NADP+NADPH | Absorption | 0.03 µM | 0.03-1 µM |
| 15259 | Amplite™ Fluorimetric Total NADP and NADPH Assay Kit *Red Fluorescence* | NADP+NADPH | Fluorescence | 0.01 µM | 0-3 µM |
| 15274 | Amplite™ Colorimetric NADP/NADPH Ratio Assay Kit | NADP/NADPH Ratio | Absorption | 0.03 µM | 0.03-1 µM |
| 15264 | Amplite™ Fluorimetric NADP/NADPH Ratio Assay Kit *Red Fluorescence* | NADP/NADPH Ratio | Fluorescence | 0.01 µM | 0-3 µM |





In the Literature

For Pricing Information Please Visit: **www.biomol.de**

Unless otherwise specified, all products are for Research Use Only.
Not for use in diagnostic or therapeutic procedures.

BIOMOL GmbH
Waidmannstraße 35 · 22769 Hamburg · Germany
info@biomol.de · www.biomol.de · www.biomol.com
Tel. 040-853 260 0 · Fax 040-853 260 22
Gebührenfrei:
Tel. 0800-246 66 51 · Fax 0800-246 66 52

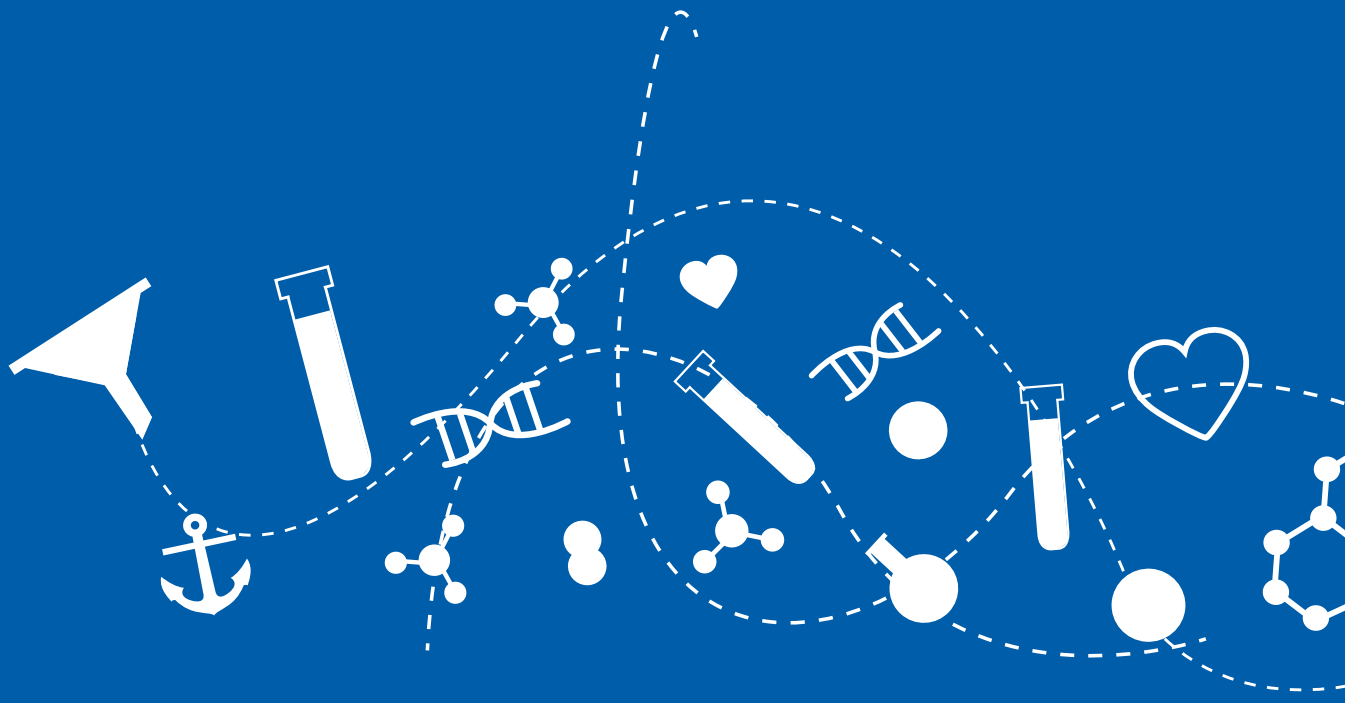

biomol

SIE HABEN DIE VISION,
WIR HABEN DIE SUBSTANZ.

2017